Available online at www.sciencedirect.com
ScienceDirect
Carbohydrate Research 343 (2008) 374–382
Carbohydrate RESEARCH

Molecular structures of glycal-based bolaamphiphiles: analysis of crystal packing and hydrogen-bond networks

Nathan C. Tice,[a] Sean Parkin[b] and Joseph J. Bozell[a,*]

[a]*Biomass Chemistry Laboratories, Forest Products Center, University of Tennessee, Knoxville, TN 37996-4570, United States*
[b]*Department of Chemistry, University of Kentucky, Lexington, KY 40506-0055, United States*

Received 9 September 2007; received in revised form 5 October 2007; accepted 9 October 2007
Available online 1 November 2007

Abstract—The crystal structures for the glycal bolaamphiphiles, 1,12-bis-(2,3-α-D-*erythro*-hex-2-enopyranosyloxy)-dodecane (**1**) and 1,12-bis-(2,3-α-D-*threo*-hex-2-enopyranosyloxy)-dodecane (**2**), were determined by single-crystal X-ray analysis. The structure for **1** showed that the α:α and α:β diastereomers co-crystallized, with occupancy factors determining an isomeric ratio of 69:31. The pyranose rings for both structures are oriented away from each other and adopt a conventional glycal geometry. The head groups are nearly *gauche* to the hydrophobic chain, which adopts an all-trans zigzag conformation. Bolaamphiphile **1** packs in anti-parallel layers, while bolaamphiphile **2** displays a parallel arrangement of layers. Both structures display a three-dimensional hydrogen-bonding network involving the hydroxylic substituents on the head groups. The high similarity in large-scale solid state structures between **1** and glucosamide bolaamphiphile **3**, and **2** and galactosamide bolaamphiphile **4** suggest a strong dependence on head group stereochemistry, and that only a few, key intermolecular interactions between head groups are necessary in controlling the ultimate structure observed. The solid state results may have implications for understanding the intermolecular forces directing nanoscale self-assembly in solution.

Keywords: X-ray; Bolaamphiphile; Crystal structure; Crystal packing; Hydrogen-bond network; Glucal, galactal; Self-assembly; Nanoscale materials

1. Introduction

Nanoscale materials have received great interest due to their potential for industrial and pharmaceutical applications.[1,2] Specifically, carbohydrate-based nanomaterials composed of glycolipids have enormous promise, as they can self-assemble in water and form highly stable mono- or bilayer membranes.[3,4] Depending upon the type of glycolipid and the conditions of self-assembly, various morphologies can arise in these systems including micelles, fibers, and tubes.[5] Vesicles or tubes composed of glycolipids could be employed in filtration and purification processes, drug delivery, and have already been used as templates for the production of synthetic inorganic materials.[3,6]

Glycolipids are composed of a long, hydrophobic (alkyl) chain, and either one (amphiphiles) or two (bolaamphiphiles) polar end groups. Regardless of the number of head groups, it is typically thought that the hydrogen-bonding networks between the polar end groups play a critical role in the physical properties, stability, and self-assembly of glycolipids.[7–9] Thus, it would follow that the more pronounced the intermolecular hydrogen bonding in amphiphiles or bolaamphiphiles, the more successful self-assembly will be. Our investigation into carbohydrate-based nanoscale materials has been primarily focused upon bolaamphiphiles incorporating glycals as head groups, for example, glucal derivative **1** and galactal derivative **2** (Fig. 1).

Predicting the topography of a self-assembled macromolecular system based on the structural and electronic features of its molecular components is still a poorly understood aspect of nanotechnology. We anticipated that the greater differentiation of the functional groups

* Corresponding author. Tel.: +1 865 974 5991; fax: +1 865 946 1109; e-mail: jbozell@utk.edu

0008-6215/$ - see front matter © 2007 Elsevier Ltd. All rights reserved.
doi:10.1016/j.carres.2007.10.026

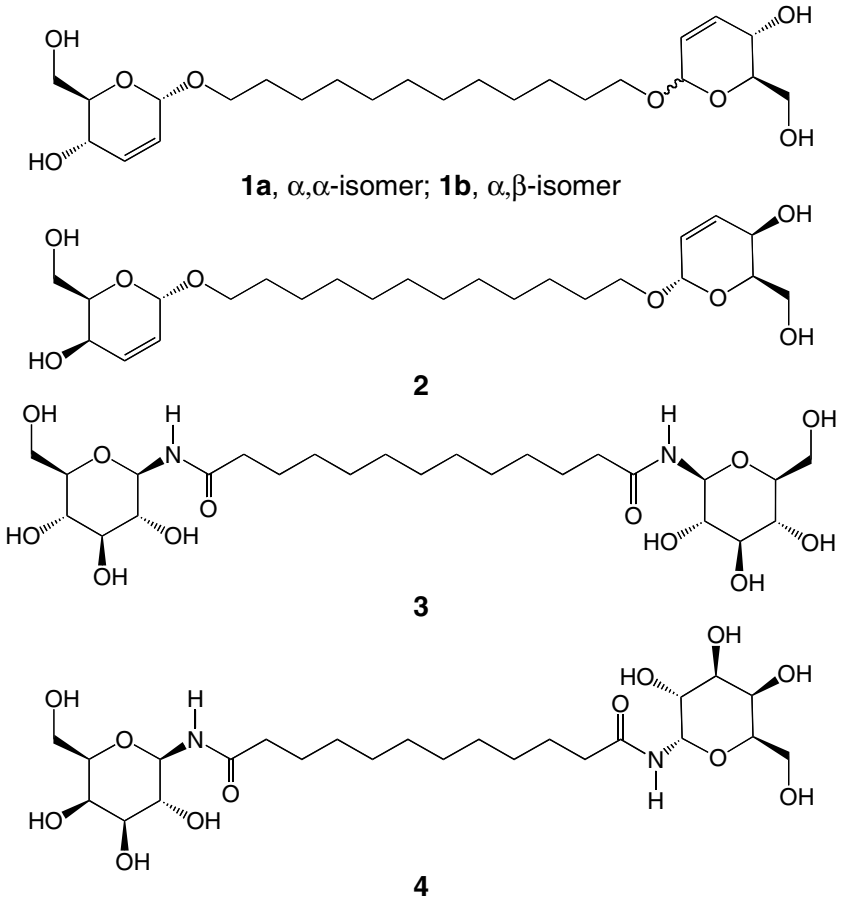

Figure 1. Glucal and carbohydrate derived bolaamphiphiles.

in glucal **1** and galactal **2** would offer an efficient means to synthesize a family of bolaamphiphiles with different head group structures, providing information on how the characteristics of the head group are manifested in the final self-assembled material. Compounds **1** and **2** are synthesized by a Ferrier reaction[10] between a long chain diol (C_8–C_{12}) and triacetylglucal or -galactal, respectively.[†] While the synthesis is relatively straightforward, a larger number of structures are observed from their self-assembly in contrast to similar bolaamphiphiles, for example, compounds containing additional alcohol and amide functionality such as glucosamide **3** or galactosamide **4** (Fig. 1).[11–15] Self-assembly of glucal-based bolaamphiphile **1** led to the presence of tubes, spheres, and larger structural bundles when observed by transmission electron microscopy, and eventually large scale aggregation to crystalline or amorphous material. We hypothesized that the reduced number of intermolecular hydrogen bonds in **1** hindered self-assembly in comparison to similar self-assembling systems such as **3** and **4**. To probe the hydrogen-bonding interaction, we characterized the glucal bolaamphiphile **1** and galactal bolaamphiphile **2** in the solid state by X-ray crystallographic analysis. Herein, we report the molecular structure of these glucal and galactal bolaamphiphiles and the analysis and comparison of their hydrogen-bonding networks.

2. Experimental

Bolaamphiphiles **1** and **2** were synthesized as described elsewhere.[†] NMR analysis shows that a bulk sample of glucal **1** comprises a mixture of both the α:α and α:β diastereomers in an approximate 70:30 ratio, whereas galactal **2** was isolated as the pure α:α isomer.

2.1. Single-crystal X-ray structural analysis

Single crystals for each sample were obtained by dissolving approximately 500 mg of material in 10 mL of hot ethanol, filtering into an Erlenmeyer flask, and allowing the solution to cool in a freezer (−20 °C) over a period of several days. The colorless, air-stable crystals isolated and used for X-ray crystallographic analysis were representative of the entire sample. These crystals were mounted on glass fibers with polyisobutene oil. Data were collected at 90 K on a Bruker-Nonius X8 Proteum

[†] Bozell, J. J.; Vidal, S.; Thompson, D.; Kim, J.-M., submitted for publication.

Table 1. Crystal data and summary of experimental details for **1** and **2**

Bolaamphiphile	**1**	**2**
Empirical formula	$C_{24}H_{42}O_8$	$C_{24}H_{42}O_8$
Formula weight	458.58	458.58
Temperature (K)	90.0(2)	90.0(2)
Wavelength (Å)	1.54178	1.54178
Crystal system, space group	Monoclinic, $P2_1$	Triclinic, $P1$
Unit cell dimensions		
a (Å)	4.8821(9)	4.9615(5)
b (Å)	44.576(8)	5.7233(6)
c (Å)	5.7778(10)	21.613(2)
α (°)	90	86.283(3)
β (°)	104.959(6)	87.476(3)
γ (°)	90	77.867(3)
Volume (Å^3)	1214.8(4)	598.45(10)
Z	2	1
Calculated density (mg/m^3)	1.254	1.272
Absorption coefficient (mm^{-1})	0.760	0.772
$F(0,0,0)$	500	250
Crystal size (mm)	$0.12 \times 0.12 \times 0.06$	$0.12 \times 0.12 \times 0.10$
θ range for data collection (°)	1.98–67.97	2.05–69.33
Limiting indices	$-5 \leqslant h \leqslant 5$, $-53 \leqslant k \leqslant 53$, $6 \leqslant l \leqslant 6$	$-6 \leqslant h \leqslant 5$, $-6 \leqslant k \leqslant 6$, $-25 \leqslant l \leqslant 25$,
Reflections collected/unique	11,536/11,536 [R(int) = 0.0704]	9000/3840 [R(int) = 0.0326]
Completeness to $\theta = 67.97$ (%)	96.0	97.7
Absorption correction	Semi-empirical from equivalents	Semi-empirical from equivalents
Max. and min. transmission	0.864 and 0.487	0.927 and 0.776
Refinement method	Full-matrix least-squares on F^2	Full-matrix least-squares on F^2
Data/restraints/parameters	11536/355/346	3840/34/300
Goodness-of-fit on F^2	1.076	1.020
Final R indices [$I > \sigma I$)]	$R_1 = 0.0713$, $wR_2 = 0.1943$	$R_1 = 0.0320$, $wR_2 = 0.0861$
R indices (all data)	$R_1 = 0.0796$, $wR_2 = 0.2039$	$R_1 = 0.0321$, $wR_2 = 0.0863$
Absolute structure parameter	0.4(3) (twinned crystal, known chirality)	0.00(4)
Extinction coefficient	0.0259(13)	0.010(2)
Largest diff. peak and hole (e Å^{-3})	0.433 and −0.466	0.264 and −0.255

diffractometer. Crystal data and a summary of experimental details are given in Table 1. The structural software used was Apex2 for cell parameters and data reduction,[16] SADABS for absorption correction,[17] SHELXL 97 for structure solution, and SHELXL 97 for refinement.[18] Restraints were applied to the disordered components to ensure similar geometries and chemically reasonable displacement parameters ('SAME', 'SIMU', and 'DELU' commands in SHELXL 97). Hydrogen atoms were placed in geometrically calculated positions.

3. Results and discussion

3.1. Molecular structure

The molecular structure and atomic labeling for the major (**1a**, α, α) and minor (**1b**, α, β) isomers of **1** is shown in Figure 2. The glucal bolaamphiphile **1** crystallizes in a monoclinic $P2_1$ space group, with two molecules in the unit cell. The crystal for **1** was twinned by a 2-fold rotation about the crystallographic a axis. Both twin components were indexed and the data integrated for each component. The absolute configuration for bolaamphiphile **1** was confirmed, with analysis showing that diastereomers **1a** and **1b** co-crystallized. The presence of two diastereomers (α:α and α:β) as indicated by NMR initially led us to believe that the major isomer would preferentially crystallize. However, occupancy factors determined that the ratio of α:α to α:β within the crystal was 69–31%, consistent with the NMR results.

The alkyl chain of glucal **1** adopts a conventional all-trans or 'zigzag' conformation. The pyranose rings for each isomer of **1** point in opposite directions and are nearly *gauche* with respect to the alkyl chain, with [O1–C1–O4–C7] and [O1′–C1′–O4′–C7′] torsion angles of 62.4° and 73.3°, respectively, for the α:α isomer and 62.4° and −80.2° for the α:β isomer. The angle between the least-squares planes for rings in the α:α isomer is 46.5° and 137.5° for the α:β isomer. Comparison of the α:α and α:β isomers of **1** (**1a** and **1b**) revealed that the disordered glycal head groups lie in roughly the same orientation, with the angle between

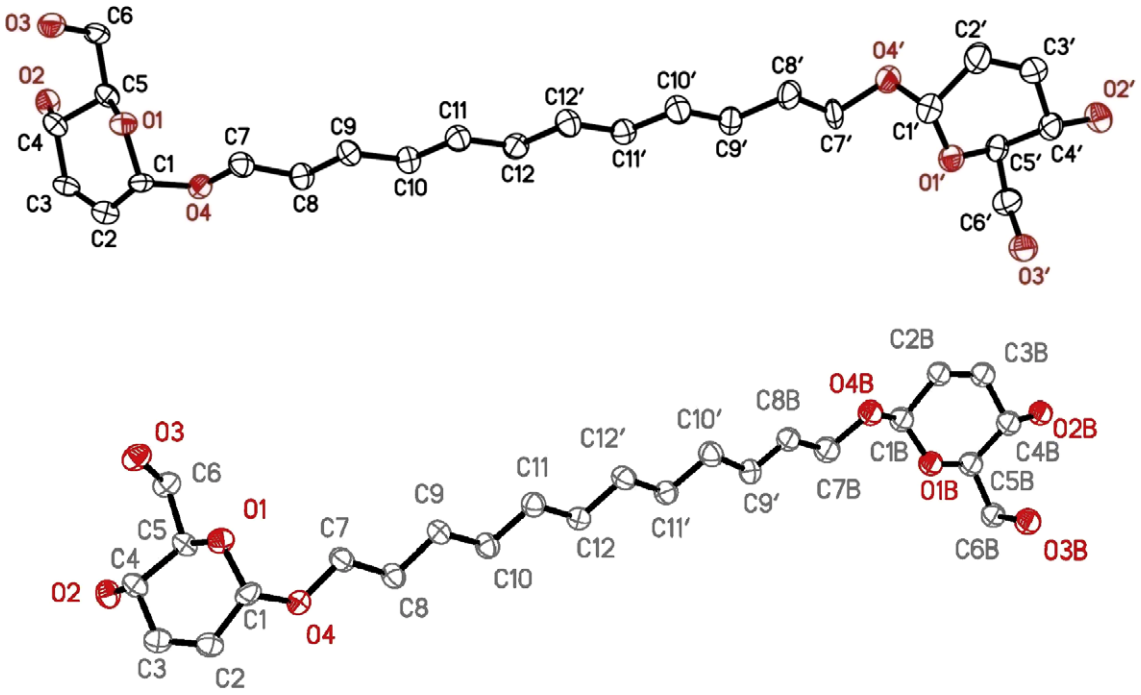

Figure 2. Molecular structure of glucal bolaamphiphile **1a and 1b**. Thermal ellipsoids are drawn at 50% probability. Hydrogen atoms have been omitted for clarity.

the least-squares planes incorporating C1′–C5′ and O1′ and C1B–C5B and O1B at 155.8°. The C–O and C–C bond lengths associated with the rings range from 1.401 to 1.542 Å and 1.475 to 1.585 Å, respectively. The average deviation from the least-squares planes for the pyranose rings for **1** is 0.186 Å. The glycal head groups adopt a conformation with the pyranose oxygen (O1, O1′, and O1B) tilted above and C5 (C5′ and C5B) below the plane of the vinyl bond (C2–C3, C2′–C3′, C2B–C3B). The [C1–O1–C5–C4] and [C1′–O1′–C5′–C4′] ([C1B–O1B–C5B–C4B]) torsion angles for each isomer are nearly identical and average 64.2°. These values correspond well with an analogous mono-glucal structure reported by Srivastava et al. (67.7°).[19]

The puckering parameters for glucal **1** and galatcal **2** are listed in Table 2.[20] The vinyl portions (C2′–C3′, and C2B–C3B′) of the disordered head group deviate significantly from idealized sp^2 geometry. The larger puckering amplitude (Q) for the disordered ring (C1′–C5′, O1′ and C1B–C5B, O1B) compared to non-disordered ring (C1–C5, O1) reflects the lower planarity of the vinyl bond (C2–C3) in the former. Double bond character is clearly evident for the C2–C3 and C2′–C3′ (C2B–C3B in **1b**) bonds for each isomer, with an average value of 1.317 Å. But the [C4–C3–C2–C1] and [C4′–C3′–C2′–C1′] ([C4B–C3B–C2B–C1B] in **1b**) torsion angles vary significantly. For the non-disordered head group (C1–C5, O1), this portion of the ring is nearly planar, with a torsion value of 0.8°. However, the double bond in the rings incorporating C1′–C5′, O1′ and C1B–C5B, O1B of **1a** and **1b** is significantly less planar, with [C4′–C3′–C2′–C1′] and [C4B–C3B–C2B–C1B] torsion angles of 15.4° and −37.4°, respectively. In contrast, the analogous torsion angle reported by Srivastava et al. of their mono-glucal structure is 2.1°,[19] reflecting a more planar arrangement of the unsaturated portion of the pyranose ring. This same deviation from idealized geometry for **1b** is observed with the [H2B–C2B–C3B–H3B] torsion angle of −37.4°. It is likely that this ability of the pyranose rings to 'relax' their conformation as needed is what gives rise to the similar packing behavior between the two diastereomers and why the isomers co-crystallize efficiently. The β portion of **1b** diverges more strongly from idealized geometry to accommodate the difference in the stereochemistry at the anomeric position (C1B) while maintaining a similar packing motif (Section 3.2) as **1a**. But, in the case of either the major or minor isomer, significant deviation from planarity may be a reflection of the drive to achieve the most efficient molecular packing or intermolecular interaction.

Table 2. Cremer–Pople puckering parameters[20] for compounds **1** and **2**

Molecule	Ring	Q (Å)	θ (°)	Φ (°)
1	C1–C5, O1	0.4739	51.78	312.98
	C1′–C5′, O1′	0.5881	65.84	296.74
	C1B–C5B, O1B	0.5384	25.55	13.76
2	C1–C5, O1	0.4425	49.93	326.97
	C1′–C5′, O1′	0.4666	52.17	329.48

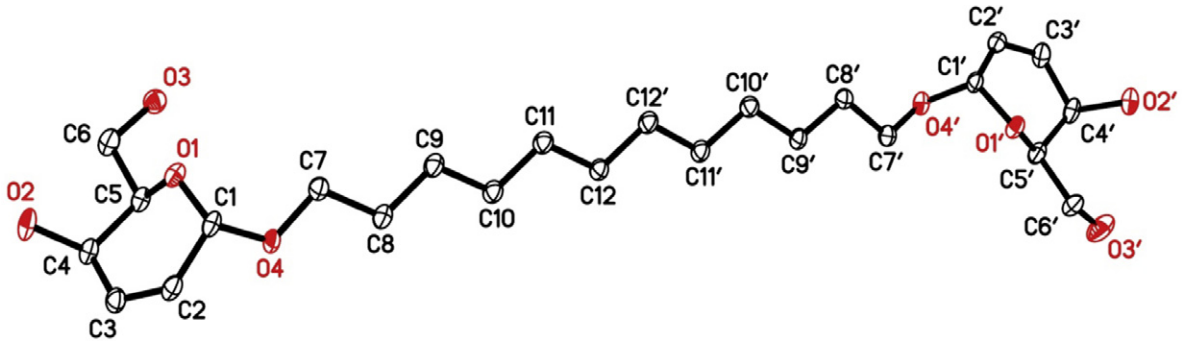

Figure 3. Molecular structure of galactal bolaamphiphile **2**. Thermal ellipsoids are drawn at 50% probability. Hydrogen atoms have been omitted for clarity.

The molecular structure for **2** is shown in Figure 3. The galactal bolaamphiphile **2** crystallizes in a triclinic *P*1 space group, with one molecule in the unit cell. The hydroxyl group incorporating O3 was found to be disordered in a difference map so a minor component was incorporated into the model. The occupancy of this minor component is small (about 10%). The absolute configuration was confirmed for **2**, with analysis showing the presence of only the α:α isomer, again consistent with NMR analysis.

Again, the alkyl chain for **2** adopts an all-trans conformation. As in the case of glucal **1**, the pyranose rings for galactal **2** point in opposite directions and are nearly *gauche* with respect to the alkyl chain, with [O1–C1–O4–C7] and [O1′–C1′–O4′–C7′] torsion angles of 64.8° and 66.8°, respectively. This orientation is also reflected in the 64.3° angle between the least-squares plane of the rings and deviates greatly from the structure of galactosamide **4**, which adopts a nearly planar ring orientation with respect to the alkyl chain.[4] In contrast, glucosamide **3** was observed to have very similar (59°) orientation of the polar head groups.[14] The pyranose rings in **2** do have a higher degree of planarity as compared to **1**, with the average deviation from the least-squares plane averaging 0.154 Å. This increased planarity is also reflected in smaller puckering amplitude (*Q*) values (Table 2), especially as compared to the disordered ring in **1**. The C–O and C–C bond lengths associated with the rings range from 1.400 to 1.429 and 1.487 to 1.517 Å, respectively. The rings adopt a conventional glycal geometry, with the pyranose oxygen (O1 and O1′) tilted above and C5 (C5′) below the plane of the vinyl bond (C2–C3 and C2′–C3′). The [C1–O1–C5–C4] and [C1′–O1′–C5′–C4′] torsion angles are 61.2° and 64.1°, respectively, again matching well with analogous values reported by Srivastava et al.[19] Double bond character is clearly evident for the C2–C3 and C2′–C3′ bonds for **2**, with values of 1.317 and 1.313 Å, respectively. However, unlike compound **1**, the vinyl bonds do not deviate strongly from sp^2 geometry. The unsaturated portions of the rings are nearly planar, with the [C4–C3–C2–C1] and [C4′–C3′–C2′–C1′] torsion angles of 0.05° and 3.0°. The [H2–C2–C3–H3] and [H2′–C2′–C3′–H3′] torsion angles are 0.01° and 3.0°, respectively, further illustrating the high degree of planarity of the vinyl bonds. Thus, for compound **2**, a relaxation from the typical glycal conformation is not necessary for efficient packing.

3.2. Molecular packing

Figures 4 and 5 show the molecular packing along the *a* and *c* axes for glucal **1a** and **1b**. Both the α:α isomer and α:β isomer display head-to-head ordered assemblies, arranged as 'pleated sheets' similar to glucosamide bolaamphiphile **3**.[14] Along both the *a* and *c* axes, each layer runs anti-parallel to the next, with the molecules viewed along the *a* axis nearly orthogonal to each other. The alkyl chains for the major and minor isomers have an inclination of 49.3° and 48.1° with respect to the normal to the layer plane, which closely matches reported values.[15] Distances between the adjacent alkyl chains are 4.97 Å (Fig. 5A) and 4.88 Å (Fig. 5B) for the major glucal isomer and 5.00 Å (Fig. 6A) and 5.23 Å (Fig. 6B) for the minor glucal isomer. These values are in close agreement with glucosamide bolaamphiphile **3** (4.92 and 6.22 Å along the *c* and *a* axes),[14] with the larger distance between pleated sheets likely arising because of the presence of the amide, which sits out of the plane of the pyranose ring. No such interaction exists in bolaamphiphiles **1** and **2**, and therefore adjacent alkyl chains can pack significantly closer. More importantly, there is little difference between the packing motifs of glucal diastereomers **1a** and **1b**. Both adopt the same anti-parallel, pleated sheet arrangement, exhibit an inclination angle of approximately 49°, and possess very similar distances between adjacent hydrophobic chains. This nearly indistinguishable packing behavior is likely why the two isomers efficiently co-crystallize. The compound can therefore be characterized as a 'solid solution' of **1b** dispersed in **1a**.

Figure 6 shows the molecular packing along the *a* and *b* axes for the galactal bolaamphiphile **2**. The packing of

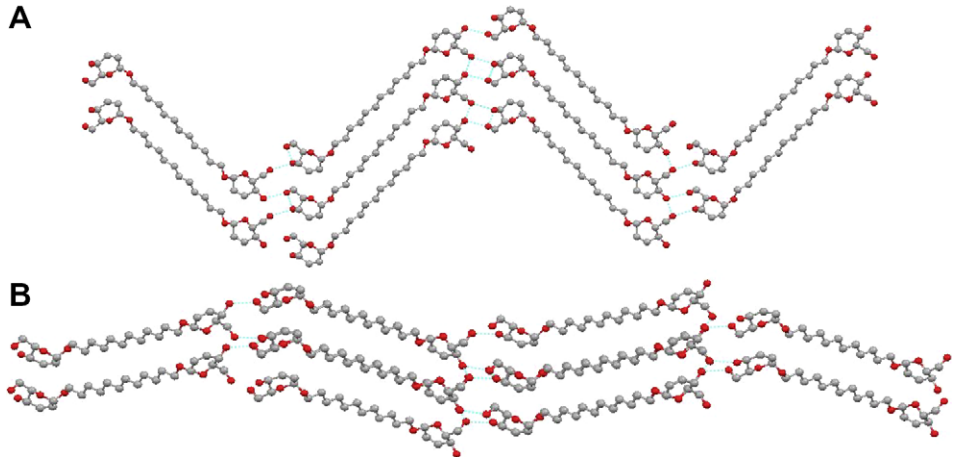

Figure 4. Molecular packing of **1** (α:α isomer) viewed along the *a* (A) and *c* (B) axis. Hydrogen atoms have been omitted for clarity.

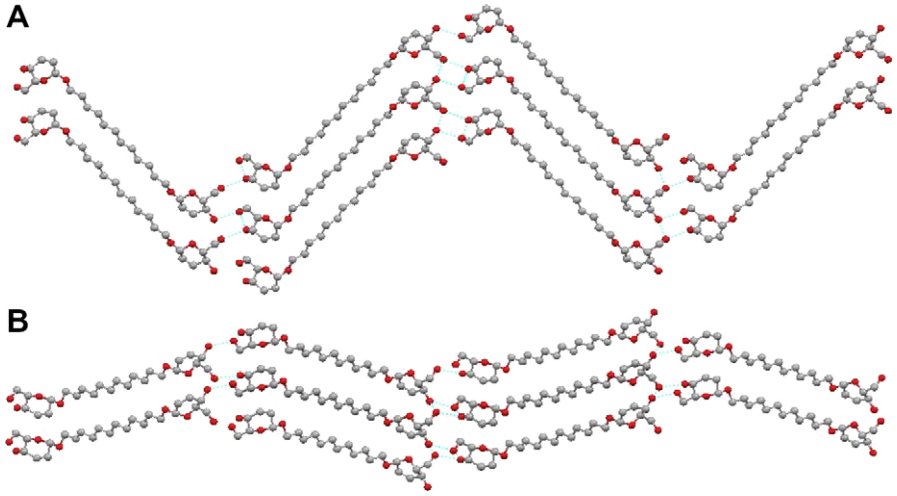

Figure 5. Molecular packing of **1** (α:β isomer) viewed along the *a* (A) and *c* (B) axis. Hydrogen atoms have been omitted for clarity.

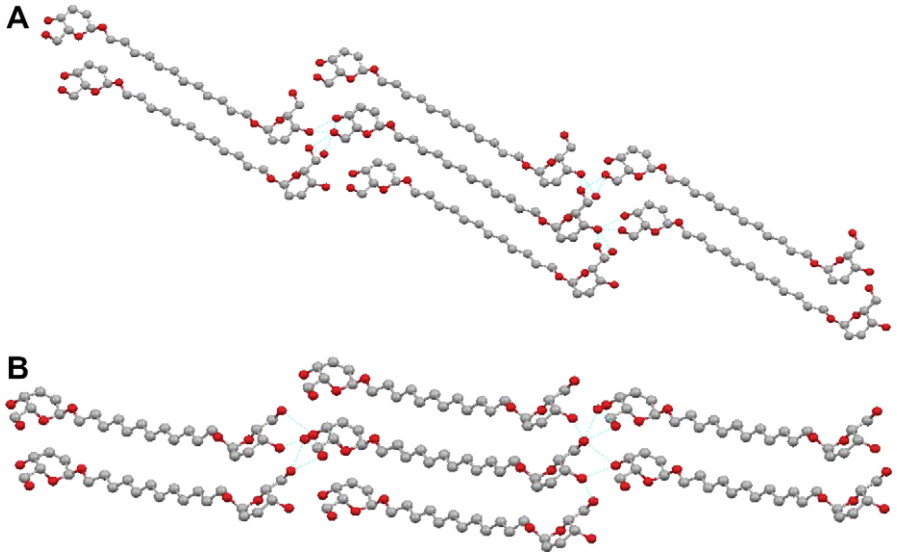

Figure 6. Molecular packing of **2** viewed along the *a* (A) and *b* (B) axis. Hydrogen atoms have been omitted for clarity.

2 displays head-to-head ordered assemblies, arranged in a parallel fashion. Similar to glucal **1**, the alkyl chain has an inclination of 49.0° with respect to the normal of the layer plane. This packing behavior is consistent with galactosamide bolaamphiphile **4**.[4,15] The major difference between our galactal case and the galactose bolaamphiphile **4** is while both cases show parallel stacking, the galactose layers in **4** are arranged in a 'staggered' fashion, with the molecule in the next layer rotated by 180° and shifted half its thickness. In the case of **2**, molecules in adjacent layers do not re-orient, but 'point' or align in the same direction. This is evident in Figure 6A and B, where each of the pyranose rings are oriented in a similar fashion, either up or down, from layer to layer. Additionally, the molecules are not staggered between sheets, but align directly above and below the molecules from adjacent layers, that is, molecules lie roughly on the same plane parallel to *bc* (Fig. 6A). Distances between alkyl chains average to 4.04 Å (Fig. 6A) and 5.07 Å (Fig. 6B). Again, these smaller distances compared to the amide bolaamphiphiles **3** and **4** occur because there is no need to accommodate a carbonyl between layers.

Overall, comparing bolaamphiphiles **1** and **2** and amide bolaamphiphiles **3** and **4**, it is striking that the packing orientation is mostly dependent upon the stereochemistry of the head group, and not the stereochemistry at the anomeric center (α vs β). When glucose/glucal is present, the molecules pack in anti-parallel pleated sheets. When galactose/galactal is employed, a parallel stacking motif is observed. Despite small differences in distances or orientations, the nature of the chain appears to have little effect on the packing.

3.3. Hydrogen-bonding network

Tables 3 and 4 display the hydrogen bonds found for structures glucal **1** and galactal **2**. It is noteworthy that **1** and **2** pack similarly to their analogs (glucosamide **3** and galactosamide **4**) in the solid state despite a significant decrease in the number and type of possible hydrogen bonding opportunities. Compound **1** displays a three-dimensional hydrogen-bonding network, which involves a total of six unique hydrogen bonds described using four molecules for each isomer (Figs. 7 and 8). In **1a**, hydrogen-bonding interactions is observed between O2–H2 and O3′, O3–H3 and O2, and O3′–H3′ and O2′. Compound **1b** has an identical hydrogen-bonding interaction between O3–H3 and O2, as well as hydrogen bonds between O3B–H3B and O2B (analogous to O3′–H3′ and O2′ in **1a**) and O2–H2 and O3B (analogous to O2–H2 and O3′ in **1a**). However, an additional hydrogen-bonding interaction is present in **1b** between O2B–H2B and O3B. The analogous interaction for **1a** (between O2′–H2′ and O3′) does not take place because H2′ is tilted too far out of the plane occupied by O2′ and O3′. This is evident by comparison of the H2′–O2′–O3′ and H2B–O2B–O3B angles of 65.3° versus 45.5°. It should be noted that for both isomers, short contact interactions (less than the sum of the Van der Waals radii) do exist between oxygen atoms that do not interact through hydrogen bonding, namely O2′ and O3 for the major isomer and O2B and O3 for the minor isomer. The distances between atoms, 2.679 Å and 2.702 Å, suggest that there may be a stabilizing interaction between these oxygens. It is interesting to note that there are no short contact interactions between the vinyl bonds in the head groups in **1a** or **1b**, indicating that no π–π interaction takes place.

As with the case for **1**, the galactal bolaamphiphile **2** displays a three-dimensional hydrogen-bonding network, which involves a total of five unique hydrogen bonds. The network can be described using four unique molecules (Fig. 9). The interactions are similar to glucal **1**, with hydrogen bonding between O2–H2 and O3, O3–H3 and O3′, O2′–H2′ and O3′, and O3′–H3′ and O2′. The fifth hydrogen bond is attributed to the disordered O3A atom, which maintains a hydrogen-bond interaction with O3′. As was the case with **1**, oxygen substituents on adjacent pyranose rings not involved in hydrogen bonding (O2 and O2′) display a close contact interaction, with the O2–O2′ distance at 2.724 Å. It is still uncertain whether this represents a legitimate stabilizing interaction in the solid state or merely a by-product of the hydrogen-bonding interaction between other alcohol substituents. Also as is the case of **1**, there are no short contact interactions between the vinyl bonds in **2**.

Table 3. Hydrogen bonds distances (Å) and angles (°) for **1** with symmetry code[a]

D–H···A	*d* (H···A)	*d* (D···A)	∠(DHA)
O2–H2···O3′ (#1)	1.86	2.688(7)	169.8
O2–H2···O3B (#1)	1.93	2.752	162.3
O3–H3···O2 (#2)	1.95	2.741(3)	156.1
O3′–H3′···O2′ (#3)	1.91	2.669(9)	149.7
O2B–H2B···O3B (#4)	2.25	2.76(3)	119.1
O3B–H3B···O2B (#3)	1.99	2.76(3)	151.9

[a] Symmetry transformations used to generate equivalent atoms: #1 $-x+2, y-1/2, -z+2$; #2 $x-1, y, z$ #3 $x, y, z+1$, #4 $x, y, z-1$.

Table 4. Hydrogen bonds distances (Å) and angles (°) for **2** with symmetry code[a]

D–H···A	*d* (H···A)	*d* (D···A)	∠(DHA)
O2–H2···O3 (#1)	1.84	2.6568(18)	163.3
O3–H3···O3′ (#2)	1.89	2.7142(19)	166.6
O3A–H3A1···O3′ (#2)	2.26	3.037(16)	154.2
O2′–H2′···O3′ (#3)	1.93	2.6693(19)	145.6
O3′–H3′···O2′ (#4)	1.91	2.6693(19)	149.0

[a] Symmetry transformations used to generate equivalent atoms: #1 $x, y+1, z$ #2 $x, y+2, z-1$ #3 $x+1, y, z$ #4 $x-1, y, z$.

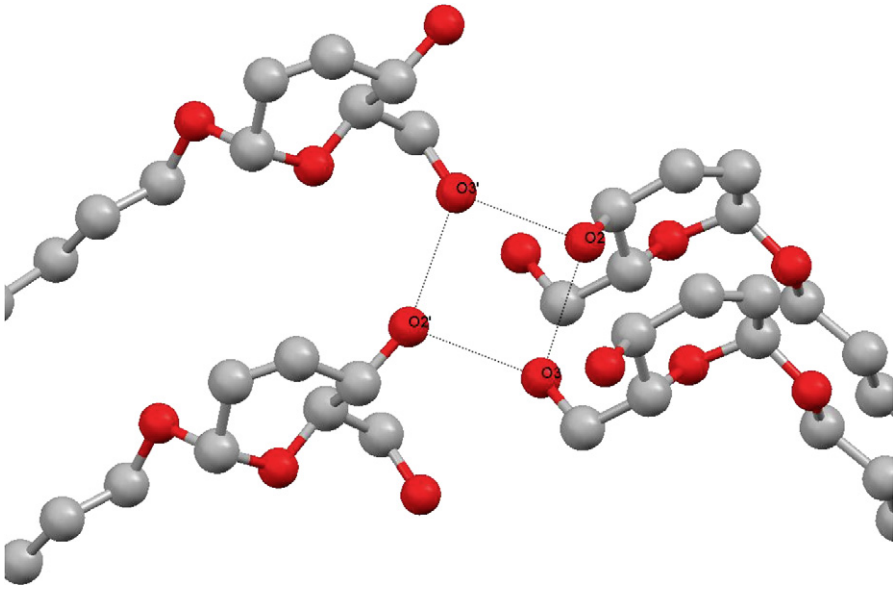

Figure 7. Close up image of hydrogen bonding and closest contacts for **1a**. Hydrogen atoms have been omitted for clarity.

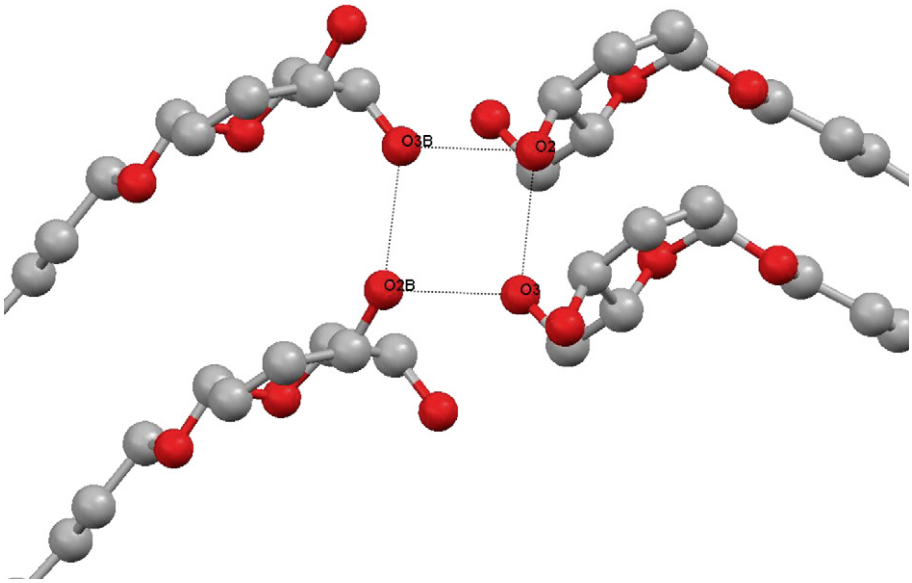

Figure 8. Close up image of hydrogen bonding and closest contacts for **1b**. Hydrogen atoms have been omitted for clarity.

The hydrogen-bonding networks for glucal **1** and galactal **2** are in stark contrast to those observed in glucosamide **3** and galactosamide **4**. The sheer number of hydrogen-bonding interactions possible in the latter systems gives the glucose and galactosamide cases a distinct advantage in self-assembly. For example, compound **4** had a total of 26 hydrogen bonds.[4] Not only do these systems have additional alcohol groups and an amide substituent available for hydrogen bonding, but also certain cases incorporate one water molecule per bolaamphiphile during packing.[4] The authors comment that the water molecules are highly involved in solid-state ordering, acting as 'glue' by hydrogen bonding with different layers of bolaamphiphile (compounds **1** and **2** exhibit poor solubility in water, and therefore had to be recrystallized in ethanol). For bolaamphiphiles **1** and **2**, the two alcohol substituents present lead to hydrogen bonded networks, but these networks are clearly not nearly as complex as those observed in the glucose and galactosamide bolaamphiphiles. This likely translates to an overall weaker hydrogen-bonding network and the lowered selectivity in self-assembly that we have observed. But in the solid state, it is still remarkable that, despite the fewer number of hydrogen-bonding interactions, both bolaamphiphiles **1** and **2** have a very similar packing motif to that of the amide bolaamphiphiles **3** and **4**. When combined with our TEM measurements,[†] these X-ray results suggest that

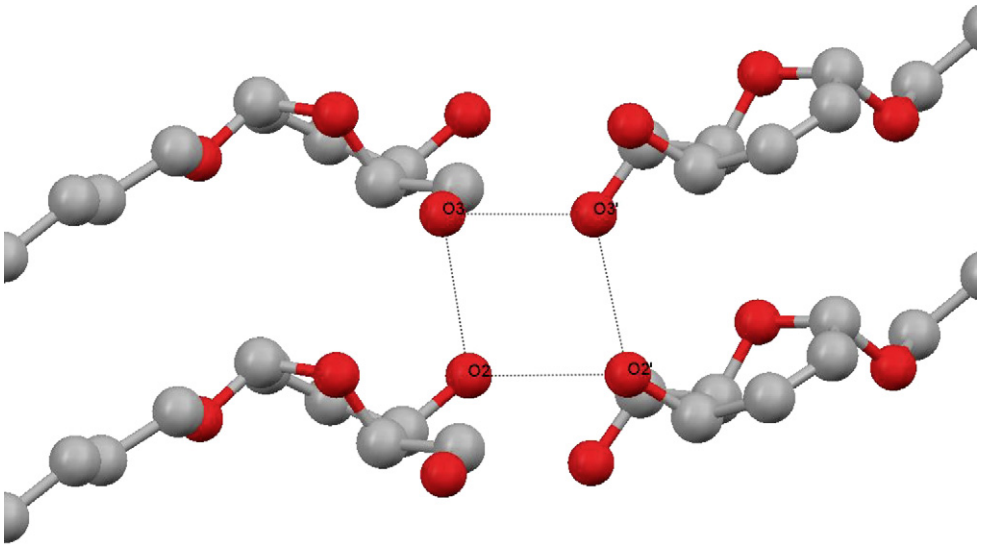

Figure 9. Close up image of hydrogen bonding and closest contacts for **2**. Hydrogen atoms have been omitted for clarity.

with respect to self-assembly, the greatly diminished number of hydrogen bonds contributes to the greater number of structures observed in solution.

However, the remaining hydrogen-bonding network is sufficient to induce an ordered crystallization. It is interesting that the large scale structure adopted in the solid state (pleated sheet or parallel plane) is the same for the glucose/glucal pair and the galactose/galactal pair, even after the hydrogen-bonding network is significantly altered. This observation suggests a strong dependence on head group stereochemistry in determining the crystalline structure, and also that only a portion of the stereochemical features present in the head group is required to direct formation of a specific solid state structure. Work is continuing to determine the impact of head group composition and stereochemistry, how the solid state results can be used to explain nanoscale self-assembly, and to understand the control of these processes in solution.

Supplementary data

Supplementary data associated with this article can be found, in the online version, at doi:10.1016/j.carres.2007.10.026.

References

1. Klabunde, K. J. *Nanoscale Materials in Chemistry*; Wiley-Interscience: New York, 2001.
2. Liz-Marzán, L. M.; Kamat, P. V. *Nanoscale Materials*; Kluwer Academic: Boston, 2003.
3. Shimizu, T.; Masuda, M.; Minamikawa, H. *Chem. Rev.* **2005**, *105*, 1401–1443.
4. Masuda, M.; Shimizu, T. *Carbohydr. Res.* **2000**, *326*, 56–66.
5. Shimizu, T. *Macromol. Rapid Commun.* **2002**, *23*, 311–331.
6. Kameta, N.; Masuda, M.; Minamikawa, H.; Goutev, N. V.; Rim, J. A.; Jung, J. H.; Shimizu, T. *Adv. Mater.* **2005**, *17*, 2732–2736.
7. Masuda, M.; Shimizu, T. *Carbohydr. Res.* **1997**, *302*, 139–147.
8. Whitesides, G. M.; Mathias, J. P.; Seto, C. T. *Science* **1991**, *254*, 1312–1319.
9. Ghadiri, M. R.; Granja, J. R.; Milligan, R. A.; Mcree, D. E.; Khazanovich, N. *Nature* **1993**, *366*, 324–327.
10. Ferrier, R. J. *Top. Curr. Chem.* **2001**, *215*, 153–175.
11. Jung, J. H.; John, G.; Yoshida, K.; Shimizu, T. *J. Am. Chem. Soc.* **2002**, *124*, 10674–10675.
12. Shimizu, T.; Masuda, M. *J. Am. Chem. Soc.* **1997**, *119*, 2812–2818.
13. Masuda, M.; Shimizu, T. *Langmuir* **2004**, *20*, 5969–5977.
14. Masuda, M.; Shimizu, T. *Chem. Commun.* **1996**, 1057–1058.
15. Shimizu, T.; Masuda, M.; Shibakami, M. *Chem. Lett.* **1997**, 267–268.
16. Bruker, APEX2 software package, Bruker AXS: 5465, East Cheryl Parkway, Madison, WI 5317, 2005.
17. Sheldrick, G. M., SADABS. University of Göttingen, Germany, 1996.
18. Sheldrick, G. M., SHELXS 97 and SHELXL 97 University of Göttingen, Germany, 1997.
19. Srivastava, R. M.; de Freitas, J. R.; da Silva, M. J.; Souto, S. C. M.; Carpenter, G. B.; Faustino, W. M. *Tetrahedron* **2004**, *60*, 10761–10769.
20. Cremer, D.; Pople, J. A. *J. Am. Chem. Soc.* **1975**, *97*, 1354–1358.